

**PULMONARY BLOOD FLOW HETEROGENEITY DURING HYPOXIA AND  
HIGH ALTITUDE PULMONARY EDEMA**

Susan R. Hopkins MD, PhD <sup>1,2</sup>, Joy Garg MD <sup>1</sup>, Divya S. Bolar BS <sup>2</sup>, Jamal Balouch BS <sup>1</sup>,  
David L. Levin MD, PhD <sup>2</sup>.

<sup>1</sup>Department of Medicine, Division of Physiology, and <sup>2</sup>Department of Radiology,  
University of California, San Diego, La Jolla, CA, USA

Correspondence and reprint requests to:  
Susan R. Hopkins MD PhD  
Department of Medicine, Division of  
Physiology 0623A  
University of California, San Diego  
9500 Gilman Dr  
La Jolla, CA, 92093  
(858)-534-2680 (tel)  
(858)-534-4812 (fax)  
shopkins@ucsd.edu

Supported by NIH HL-17731, NIH MO1-RR00827

Running head; pulmonary blood flow and HAPE.

Word count:3184

Descriptor Number 148 High Altitude

This article has an online data supplement which is accessible from this  
issue's table of contents at [www.atsjournals.org](http://www.atsjournals.org)

## **ABSTRACT**

Uneven hypoxic pulmonary vasoconstriction has been proposed to expose parts of the pulmonary capillary bed to high pressure and vascular injury in high altitude pulmonary edema. We hypothesized that subjects with a history of high altitude pulmonary edema would demonstrate increased heterogeneity of pulmonary blood flow during hypoxia. A functional magnetic resonance imaging technique (arterial spin labeling), was used to quantify spatial pulmonary blood flow heterogeneity in 3 subject groups: 1) Susceptible (n=5), history of physician documented high altitude pulmonary edema; 2) Resistant (n=6), repeated high altitude exposure without illness, 3) Unselected (n=6), minimal history of altitude exposure. Data were collected in normoxia and after 5, 10, 20 and 30 minutes of normobaric hypoxia ( $FIO_2 = 0.125$ ). Relative dispersion (standard deviation/mean) of the signal intensity was used as an index of perfusion heterogeneity. Oxygen saturation was not different between groups during hypoxia. Relative dispersion was not different between groups ( $0.94 \pm 0.05$  Susceptible,  $0.94 \pm 0.05$  Resistant,  $0.87 \pm 0.06$  Unselected, means  $\pm$  SEM) during normoxia, but it was increased by hypoxia in Susceptible (to  $1.10 \pm 0.05$  after 30 min,  $p < 0.0001$ ) but not in Resistant ( $0.91 \pm 0.05$ ) or Unselected subjects ( $0.87 \pm 0.05$ ). Susceptible individuals have increased pulmonary blood flow heterogeneity in acute hypoxia, consistent with uneven hypoxic pulmonary vasoconstriction.

## **KEY WORDS**

Magnetic resonance imaging, pulmonary circulation, hypoxic pulmonary vasoconstriction

Abstract word count: 200 words.

## INTRODUCTION

High altitude pulmonary edema (HAPE) is a non-cardiogenic high permeability edema, characterized by alveolar fluid with a high concentration of protein (1) that develops in otherwise healthy individuals following 24-72 hours exposure to altitudes above 2400 m (~8000 feet). Typically, radiographs in HAPE demonstrate a patchy distribution of edema, appearing first in the perihilar regions of the lung (2). The reported incidence is 2-15% of exposed individuals depending on rate of ascent and altitude reached (3-5). Risk factors include rapid ascent, strenuous exercise, and a previous history of HAPE. Increased pulmonary artery pressure is a hallmark of HAPE (6, 7), and susceptible subjects have been shown to have increased pulmonary arterial pressures prior to the development of HAPE (8). Increased concentrations of red blood cells and protein in bronchoalveolar lavage fluid are observed in the early stages of HAPE before inflammatory cytokines are present (9), suggesting that mechanical injury to the pulmonary capillary bed (stress failure) may be important in the development of HAPE. Since hypoxic pulmonary vasoconstriction takes place in the pre-capillary arterioles it is uncertain how capillaries might be exposed to high pressure. A mechanism initially proposed by Visscher (10) and later modified for HAPE by Hultgren (reviewed in (2)) is that hypoxic pulmonary vasoconstriction is uneven in HAPE (2). If this were true, some parts of the capillary bed would be protected by upstream vasoconstriction, whereas the portions of the capillary that did not have upstream vasoconstriction would be exposed to high pressures and mechanical stress injury(11), thus inciting HAPE.

Recent animal work confirms that hypoxia results in increased spatial heterogeneity of pulmonary perfusion, suggesting that hypoxic pulmonary vasoconstriction is inherently uneven in the mammalian lung (12). However, the relationship between the development of uneven hypoxic pulmonary vasoconstriction and susceptibility to HAPE is unknown, and it is uncertain whether HAPE susceptible subjects have increased heterogeneity of pulmonary perfusion in response to hypoxia. We hypothesized that HAPE susceptible subjects would demonstrate increased pulmonary blood flow heterogeneity during hypoxia compared to subjects without a history of HAPE. To test this hypothesis, we measured pulmonary blood flow heterogeneity in response to acute hypoxia using a quantitative magnetic resonance imaging (MRI) technique known as arterial spin labeling. Arterial spin labeling involves creating a magnetically tagged bolus by the use of specialized radiofrequency pulses to alter the magnetization of water in

blood. By measuring the transit of the tagged bolus through organ vasculature, it is possible to measure the spatial distribution of blood flow. Arterial spin labeling has been widely applied to measure cerebral blood flow (13), and to a lesser extent has been used to evaluate perfusion in skeletal muscle (14), heart (15), kidney (16), and lung(17). We measured the distribution of pulmonary blood flow using arterial spin labeling in normoxia and acute hypoxia in subjects with a history of HAPE and compared the results to individuals repeatedly exposed to altitude without HAPE, and subjects unselected for HAPE-susceptibility by virtue of very limited high altitude exposure. Some of the results of this study been previously reported in the form of an abstract (18, 19).

### **CONDENSED METHODS**

The Human Subjects Research Protection Program of the University of California San Diego approved this study, and the procedures followed conformed with this institution's guidelines. Healthy nonsmoking subjects were recruited by advertisement, informed of the risks of the study, and signed informed consent. A history was taken, with particular reference to the cardiopulmonary system and history of altitude exposure, and a physical examination was performed. The subjects were recruited from 3 groups: HAPE susceptible, with a history of physician documented HAPE on at least one occasion, (n = 5); HAPE resistant, repeated high altitude exposure > 5,400m, without any history of altitude illness, (n = 6), and Unselected subjects, with very limited altitude exposure history (see results, n = 6).

The subjects were screened for cardiac (EKG) and pulmonary abnormalities (chest radiograph, spirometry) Each subject underwent MR imaging with arterial spin labeling using a Vision 1.5 T whole-body MR Scanner (Siemens Medical Systems, Erlangen, Germany). MRI arterial spin labeling is a clinical technique used for the quantification of organ blood flow. The signal intensity of the image has been shown to be proportional to bulk flow *in vitro* using a tube-flow model (20) and it has been validated in heart (15) with microspheres, and skeletal muscle with venous occlusion plethysmography (21) with an excellent linear relationship between arterial spin labeling measurements and the validating technique. Arterial spin labeling inverts the proton magnetization of blood by applying a radiofrequency pulse, allowing these magnetically tagged protons in blood to act as an endogenous tracer for the evaluation of blood flow (see online data supplement Figures E1 and E2). During each measurement two images are acquired.

In the first image, an inversion pulse is applied to the entire volume of the lungs and the image of the selected lung slice is taken. In the second image, a second inversion pulse is used, but applied ONLY to the image slice (a selective inversion). During the delay before the second image is acquired, any blood that enters the image slice from outside will have been missed by the selective inversion. The two images are then subtracted. Since stationary inverted protons from tissue will be present in both images, they will cancel one another out. Thus the signal from each image voxel is then proportional to the amount of blood that entered the voxel in the delay between the selective inversion pulse and the image acquisition. The sequence is cardiac gated and flow data are collected over one cardiac cycle encompassing one systole and portions of two diastoles.

Subjects rested in the supine position wearing a face mask (Hans Rudolph 8930, Kansas City, MO), equipped with a non-rebreathing valve (Hans Rudolph 2700, Kansas City, MO). Pulmonary perfusion was quantified using a cardiac gated pulmonary arterial spin labeling magnetic resonance sequence as described (17). A detailed description of these methods is given in the online data supplement. All sequence parameters were kept within FDA guidelines for clinical MR examinations. The spatial resolution of measurement with this technique is  $1.5 \times 3 \times 15 \text{ mm}$  ( $\sim 70 \text{ mm}^3$ ).

Data were obtained during a 8-10 second breath-hold at functional residual capacity in a 15 mm thick image slice in the coronal plane in the posterior one-third of the lung using the posterior edge of the descending aorta as a reference point. Five measures were obtained at each time point and averaged. Baseline data were obtained after resting quietly in the magnet for 10 minutes breathing room air. Then, the inspired port of the Hans Rudolph valve was connected to a Douglas bag containing a  $\text{FIO}_2 = 0.125$  ( $\sim 3800\text{m}$  equivalent altitude) and data collection was repeated after 5, 10, 20, and 30 minutes of hypoxia. Arterial oxygen saturation and heart rate were monitored (3150 MR Monitor, Invivo Research Inc. Orlando, FL). The signal intensity for each voxel within the lung parenchyma was determined for each image using MATLAB (The MathWorks, Natick, MA). Relative dispersion (standard deviation/mean signal intensity), an index of blood flow heterogeneity where a greater number indicates a more heterogeneously distributed system, was calculated for all time points (22). Figure 1 presents reliability data for relative dispersion of perfusion heterogeneity obtained in 45 healthy nonsmoking volunteers

using MRI arterial spin labeling.

Data were analyzed using ANOVA (Statview 4.1, SAS Institute Inc. Cary, NC) with one randomized group (subject Group, 3 levels, HAPE-susceptible, HAPE-resistant and Unselected subjects) and one repeated measure (duration of Hypoxia 5 levels 0, 5, 10, 20, and 30 minutes) (23, 24). Where overall significance was determined, post hoc ANOVA testing was applied to determine where the differences occurred. Linear regression was used to relate the change in blood flow heterogeneity to arterial oxygen saturation(24). Significance was accepted at  $P < 0.05$ , 2 tailed. All data are means  $\pm$  SEM.

## RESULTS

Subject descriptive data are given in Table 1. Four of the five HAPE-susceptible subjects were diagnosed on the basis of chest radiographs in addition to history and physical findings. The remaining subject had a classic history for HAPE, in addition to typical physical findings, which were documented by his physician. Three of our HAPE-susceptible subjects were experienced climbers: two had experienced HAPE on more than one occasion, and the third had experienced HAPE on one occasion after a rapid ascent. All three of these individuals continued to travel to high altitude regularly. The other two HAPE-susceptible subjects had developed HAPE on their first time at altitude and had not returned to high altitude because of concerns over a reoccurrence. All of the HAPE-resistant subjects were experienced alpinists, and regularly traveled to high altitude, usually with very rapid ascent profiles. Four of this group had Himalayan climbing experience; one had guided a successful climb of Mt. Everest (8848 M). The remaining 2 had climbed in South America. One subject in the Unselected group had a single history of brief exposure to an altitude of 4300 m 2 years prior to the study. The remaining subjects had not travelled above 2400-4000m and all exposures at these altitudes were more than one year prior to the study, of brief (few hours) duration, with no overnight stay, and on a single occasion only. None had slept above 2000m.

There were no significant differences between groups for age, height, weight, or pulmonary function variables (Table 1). The HAPE-resistant subjects had reached significantly higher altitudes ( $6736 \pm 460$  m) than either the HAPE-susceptible ( $5907 \pm 678$  m) or the Unselected subjects ( $3322 \pm 299$  m). Arterial oxygen saturation (Figure 2, top) was  $98.2 \pm 0.2\%$  at baseline and fell to  $87.2 \pm 1.3\%$  after 30 minutes of hypoxia ( $P < 0.0001$ ) but there were no significant

differences between groups ( $P = 0.56$ ) and no significant group by time interaction ( $P = 0.77$ ), thus all subject groups experienced a similar level of hypoxia. Heart rate (Figure 2 bottom) measured by pulse oximetry was increased by hypoxia ( $P < 0.0001$ ), however this was not significantly different between groups ( $P = 0.57$ ), and there was no significant group by time interaction ( $P = 0.63$ ).

The overall quality of the MRI perfusion maps was excellent and mean signal to noise ratio was 29:1. The mean signal did not differ between the three subject groups over the course of the study. The relative dispersion of signal intensity (Figure 3) was not different between groups at baseline ( $0.94 \pm 0.05$  HAPE-susceptible;  $0.94 \pm 0.05$  HAPE-resistant;  $0.87 \pm 0.06$  Unselected subjects). However, relative dispersion was increased during hypoxia in HAPE-susceptible (to  $1.10 \pm 0.05$  after 30 min,  $P < 0.0001$ ) but not in HAPE-resistant ( $0.91 \pm 0.05$ ,  $P = 0.44$ ) or Unselected subjects ( $0.87 \pm 0.05$ ,  $P = 0.30$ ). Strikingly, all of the HAPE-susceptible subjects increased pulmonary blood flow heterogeneity by at least 10% of their baseline values by 30 minutes of hypoxia (Figures 4 and 5).

Since there was no difference in the change in relative dispersion in response to hypoxia between the HAPE-resistant and Unselected subjects, these data were pooled and linear regression was performed. There was a significant relationship between arterial oxygen saturation at 30 minutes and the change in relative dispersion from baseline (Figure 4,  $R = -0.60$ ,  $P < 0.05$ ). Overall, hypoxia was associated with small reductions in relative dispersion in these subjects, but three of the subjects who became the most hypoxic had small increases in heterogeneity resulting in a negative slope. When data from the 5 HAPE-susceptible subjects were plotted on the same Figure, all of the values for the change in relative dispersion HAPE-susceptible subjects fell above the + 2 SD confidence limits for the relationship of the change in relative dispersion verses arterial oxygen saturation. Additionally, there was a strong within subject relationship between arterial oxygen saturation and relative dispersion for the HAPE-susceptible subjects, with an average correlation of  $-0.82$  within subjects across all time points (Figure 5). By contrast the correlation between saturation and relative dispersion averaged  $+0.17$  for the HAPE-resistant subjects and  $-0.01$  for the unselected subjects.

## DISCUSSION

We describe a highly significant difference in the pulmonary vascular response to hypoxia between HAPE-susceptible individuals and those who have not suffered from HAPE. Clearly, we can not determine whether this finding is a predisposing factor for, or a consequence of, having had HAPE. During hypoxia, all of the HAPE-susceptible subjects demonstrated an increase in pulmonary blood flow heterogeneity as measured by the relative dispersion of MRI signal intensity of at least 10% of baseline values. Although 2 of the other subjects, one Unselected subject and one HAPE-resistant subject, had a small increases in pulmonary blood flow heterogeneity during hypoxia, these were ~ one half of the smallest response seen in any of the HAPE-susceptible subjects and were not significantly different from zero.

There are several factors that might affect the absolute quantification of regional pulmonary blood flow *in vivo*. All flowing blood that enters the image plane from outside the selective tag region– from both arteries and veins – will contribute to the signal intensity of the perfusion-weighted image, thus changes in the heterogeneity of signal intensity could reflect alterations in local arterial blood flow, venous blood flow, or both. Also, the physical width of the tagging slice is greater than that of the imaging slice. This creates a gap through which protons in blood must travel prior to being imaged. Since some of the protons tagged within flowing blood may not reach the imaging slice, this may result in an underestimation of total blood flow, particularly in low velocity vessels. As data is collected for one systolic period, a small amount of flow during diastole will be excluded. However, it is unlikely that these factors that potentially affect the absolute quantification of flow, and almost certainly the heterogeneity of flow would be altered by significantly by hypoxia *per se*.

The study was designed to minimize the potential impact of these factors. Subjects remained in the same position in the magnet for the duration of the study. For each subject, the imaging parameters were held constant, the same anatomic level was used for all measurements, and all three subject groups followed the identical imaging protocol. Blood flow data were collected from a single anatomic location across multiple breath-holds. Each subject was trained to achieve a consistent breath-hold volume, which was verified on the anatomic images obtained. In addition this technique is highly reliable (Figure 1), thus changes are unlikely to be the result of a random variability. Importantly, this study did not seek to quantify absolute flow, but

quantified flow heterogeneity within a subject. By using each subject as his or her own control, while there may be some error in estimation of absolute pulmonary blood flow, the magnitude of any error will be constant within a subject across time. Most importantly, the calculation of relative dispersion should significantly reduce the importance of any errors in quantification of absolute flow, as these potential errors should affect all vessels within the same subject in a relatively uniform fashion, and should not change during the study. Thus the observed changes in relative dispersion in the HAPE-susceptible subjects correspond directly to changes in the uniformity of regional pulmonary blood flow. It is unlikely that these differences in the pulmonary vascular response are related to ongoing altitude exposure in an particular subject group since increased perfusion heterogeneity was observed in all of the HAPE-susceptible subjects irrespective of recent altitude exposure and was not observed in either the HAPE-resistant subjects, who continued to travel to altitude regularly, or the Unselected subjects, who had very limited lifetime exposure to altitude and had not traveled above 3000m in the last year.

The factors that determine an individual's susceptibility to HAPE are poorly understood (reviewed in (2, 5)). HAPE-susceptible subjects have been shown to have exaggerated hypoxic pulmonary vasoconstriction compared to HAPE-resistant subjects (7, 25-27), greater resting pulmonary vascular resistance (28), and higher pulmonary arterial and capillary wedge pressures (28) during exercise. In addition, it has been shown that capillary pressures are increased in HAPE-susceptible during hypoxic exposure (29). These increased pulmonary vascular pressures are important because there is evidence that pulmonary capillaries suffer mechanical damage during heavy exercise (30, 31) and recent evidence indicates that damage to the capillary endothelium precedes the development of the leak in HAPE (9). How the pulmonary capillaries are exposed to increased microvascular pressure has been uncertain, since the site of vasoconstriction is proximal to the vulnerable capillary bed, leading to the hypothesis that hypoxic pulmonary vasoconstriction is uneven in HAPE.

Although uneven pulmonary blood flow (10) resulting from uneven hypoxic pulmonary vasoconstriction (2) has long been postulated as an important mechanism in HAPE, direct evidence for this idea has been difficult to obtain, largely because of the lack of appropriate tools to measure regional pulmonary blood flow in humans. In pigs (12), recent work using fluorescent microspheres has demonstrated that hypoxic pulmonary vasoconstriction is inherently non-uniform. In these animals, a particular vasoconstrictive response is distributed among anatomic

regions of the lung, and areas of relatively high flow during hypoxia tend to be adjacent to other areas of high flow, while low flow areas are clustered near other low flow areas. Also, there is an apparent influence of regional ventilation perfusion ratio, and areas of low ventilation perfusion ratio tend to vasoconstrict at a higher inspired oxygen concentration than areas of high ventilation-perfusion ratio. In HAPE-susceptible humans, hypoxia is associated with a shift of pulmonary perfusion, to the apical region of the lung as measured by ventilation-perfusion scintigraphy (32). This regional shift in blood flow was not seen in control subjects. However, since HAPE susceptible subjects are well known to experience higher pulmonary vascular pressures during hypoxia, this would be expected to recruit reserve vessels resulting in a more even overall distribution of pulmonary blood flow, accounting for the apical shift in perfusion. Thus, based on these previous findings, it is been difficult to distinguish the effects of pressure on pulmonary blood flow distribution from uneven hypoxic pulmonary vasoconstriction.

We found an increase in pulmonary blood flow heterogeneity in the HAPE-susceptible subjects when they were exposed to hypoxia. This was not observed in either of the other subject groups. The extent that this heterogeneity contributes to the pathogenesis is uncertain, particularly in light of the short duration of the hypoxic exposure in this study. Although HAPE-susceptible subjects develop higher pulmonary vascular pressures when exposed to hypoxia, the changes in flow heterogeneity we observed in our HAPE-susceptible subjects are not likely to reflect higher pulmonary vascular pressures alone, since a increase in pressure would be expected to cause recruitment of blood vessels and more uniform blood flow rather than less uniform pulmonary blood flow. More likely, these changes in perfusion heterogeneity reflect a more heterogeneous pattern of hypoxic pulmonary vasoconstriction in the HAPE-susceptible subjects. Whether this difference reflects a greater heterogeneity in the stimulus, regional alveolar  $PO_2$  or the response to the stimulus, secondary to heterogeneity in the pulmonary vascular distribution of smooth muscle, is an intriguing but unresolved issue. Irrespective of mechanism, these data are consistent with the hypothesis that uneven hypoxic pulmonary vasoconstriction may play a role in the development of HAPE, and could explain how high vascular pressures develop in the pulmonary capillaries in HAPE-susceptible individuals.

## **ACKNOWLEDGMENTS**

We thank the subjects for their enthusiastic participation. We would like to thank Rick Buxton, Tom Liu, Eric Wong, and Larry Frank for their assistance with the pulse sequence programming and discussions regarding the MRI ASL-FAIRER measurements of regional pulmonary blood flow. We also would like to thank an anonymous reviewer who drew our attention to the work of Maurice Visscher, who described the potential role of uneven pulmonary blood flow in the development of pulmonary edema (10, 33).

## REFERENCES

1. Schoene RB, Hackett PH, Henderson WR, Sage EH, Chow M, Roach RC, Mills WJ, Martin TR. High-altitude pulmonary edema. Characteristics of lung lavage fluid. *JAMA* 1986;256:63-69.
2. Hultgren HN. *High Altitude Medicine*. Stanford, CA: Hultgren Publications; 1997.
3. Hackett PH, Rennie D. The incidence, importance, and prophylaxis of acute mountain sickness. *Lancet* 1976;2:1149-1155.
4. Cremona G, Asnaghi R, Baderna P, Brunetto A, Brutsaert T, Cavallaro C, Clark TM, Cogo A, Donis R, Lanfranchi P, et al. Pulmonary extravascular fluid accumulation in recreational climbers: a prospective study. *Lancet* 2002;359:303-309.
5. Schoene R, Swenson E, Hultgren H. High Altitude Pulmonary Edema. In: Hornbein T, Schoene R, editors. *High Altitude. An exploration of human adaptation*. New York: Marcel Dekker Inc.; 2001. p. 777-814.
6. Hultgren HN, Lopez CE, Lundberg E, Miller H. Physiologic Studies of Pulmonary Edema at High Altitude. *Circulation* 1964;29:393-408.
7. Hultgren HN, Grover RF, Hartley LH. Abnormal circulatory responses to high altitude in subjects with a previous history of high-altitude pulmonary edema. *Circulation* 1971;44:759-770.
8. Bartsch P, Maggiorini M, Ritter M, Noti C, Vock P, Oelz O. Prevention of high-altitude pulmonary edema by nifedipine. *N Engl J Med* 1991;325:1284-1289.
9. Swenson ER, Maggiorini M, Mongovin S, Gibbs JS, Greve I, Mairbaurl H, Bartsch P. Pathogenesis of high-altitude pulmonary edema: inflammation is not an etiologic factor. *JAMA* 2002;287:2228-2235.
10. Visscher MB. Studies on embolization of lung vessels. *Med Thorac* 1962;19:334-340.

11. Hultgren HN. Pulmonary hypertension and pulmonary edema. In: Loeppky JA, Riedesel ML, editors. Oxygen transport to human tissue. New York: Elsevier/North Holland; 1982. p. 243-254.
12. Hlastala MP, Lamm WJ, Karp A, Polissar NL, Starr IR, Glenny RW. Spatial Distribution of Hypoxic Pulmonary Vasoconstriction in the Supine Pig. *J Appl Physiol* 2003;29:29.
13. Wong EC, Buxton RB, Frank LR. Quantitative imaging of perfusion using a single subtraction (QUIPSS and QUIPSS II). *Magn Reson Med* 1998;39:702-708.
14. Frank LR, Wong EC, Haseler LJ, Buxton RB. Dynamic imaging of perfusion in human skeletal muscle during exercise with arterial spin labeling. *Magn Reson Med* 1999;42:258-267.
15. Poncelet BP, Koelling TM, Schmidt CJ, Kwong KK, Reese TG, Ledden P, Kantor HL, Brady TJ, Weisskoff RM. Measurement of human myocardial perfusion by double-gated flow alternating inversion recovery EPI. *Magn Reson Med* 1999;41:510-519.
16. Roberts DA, Detre JA, Bolinger L, Insko EK, Lenkinski RE, Pentecost MJ, Leigh JS, Jr. Renal perfusion in humans: MR imaging with spin tagging of arterial water. *Radiology* 1995;196:281-286.
17. Mai VM, Berr SS. MR perfusion imaging of pulmonary parenchyma using pulsed arterial spin labeling techniques: FAIRER and FAIR. *J Magn Reson Imaging* 1999;9:483-487.
18. Levin D, Garg J, Bolar D, Balouch J, Hopkins S. Pulmonary Blood Flow Heterogeneity During Hypoxia Measured with ASL-FAIRER in Subjects with Prior High Altitude Pulmonary Edema (HAPE). *Proc Intl Soc Mag Reson Med 12th meeting* 2004:644.
19. Garg J, Levin D, Bolar D, Hopkins S. Pulmonary blood flow heterogeneity during hypoxia in subjects with a history of high altitude pulmonary edema (HAPE). *High Altitude Med Biol* 2003;4:429.
20. Andersen IK, Sidaros K, Gesmara H, Rostrup E, Larsson HB. A model system for perfusion quantification using FAIR. *Magn Reson Imaging* 2000;18:565-574.

21. Raynaud JS, Duteil S, Vaughan JT, Hennel F, Wary C, Leroy-Willig A, Carlier PG. Determination of skeletal muscle perfusion using arterial spin labeling NMRI: validation by comparison with venous occlusion plethysmography. *Magn Reson Med* 2001;46:305-311.
22. Glenny RW. Heterogeneity in the lung: concepts and measures. In: Hlastala MP, Robertson HT, editors. *Complexity in structure and function in the lung*. New York: Marcel Dekker Inc.; 1998. p. 571-609.
23. Kusuoka H, Hoffman JI. Advice on statistical analysis for Circulation Research. *Circ Res* 2002;91:662-671.
24. Glantz SA, Slinker BK. *Primer of applied regression and analysis of variance*. second ed. New York: McGraw-Hill Inc.; 2001.
25. Kawashima A, Kubo K, Kobayashi T, Sekiguchi M. Hemodynamic responses to acute hypoxia, hypobaria, and exercise in subjects susceptible to high-altitude pulmonary edema. *J Appl Physiol* 1989;67:1982-1989.
26. Viswanathan R, Jain SK, Subramanian S, Subramanian TA, Dua GL, Giri J. Pulmonary edema of high altitude. II. Clinical, aerohemodynamic, and biochemical studies in a group with history of pulmonary edema of high altitude. *Am Rev Respir Dis* 1969;100:334-341.
27. Yagi H, Yamada H, Kobayashi T, Sekiguchi M. Doppler assessment of pulmonary hypertension induced by hypoxic breathing in subjects susceptible to high altitude pulmonary edema. *Am Rev Respir Dis* 1990;142:796-801.
28. Eldridge MW, Podolsky A, Richardson RS, Johnson DH, Knight DR, Johnson EC, Hopkins SR, Michimata H, Grassi B, Feiner J, et al. Pulmonary hemodynamic response to exercise in subjects with prior high-altitude pulmonary edema. *J Appl Physiol* 1996;81:911-921.

29. Maggiorini M, Melot C, Pierre S, Pfeiffer F, Greve I, Sartori C, Lepori M, Hauser M, Scherrer U, Naeije R. High-Altitude Pulmonary Edema Is Initially Caused by an Increase in Capillary Pressure. *Circulation* 2001;103:2078-2083.
30. Hopkins SR, Schoene RB, Henderson WR, Spragg RG, Martin TR, West JB. Intense exercise impairs the integrity of the pulmonary blood-gas barrier in elite athletes. *Am J Respir Crit Care Med* 1997;155:1090-1094.
31. West JB, Mathieu-Costello O, Jones JH, Birks EK, Logemann RB, Pascoe JR, Tyler WS. Stress failure of pulmonary capillaries in racehorses with exercise-induced pulmonary hemorrhage. *J Appl Physiol* 1993;75:1097-1109.
32. Hanaoka M, Tanaka M, Ge R-L, Droma Y, Ito A, Miyahara T, Koizumi T, Fujimoto K, Fujii T, Kobayashi T, et al. Hypoxia-Induced Pulmonary Blood Redistribution in Subjects With a History of High-Altitude Pulmonary Edema. *Circulation* 2000;101:1418-1422.
33. Visscher MB. Normal and Abnormal Pulmonary Circulation. Paper presented at: 5th Conference on Research in Emphysema; 1962, 1962; Aspen, CO.

## FIGURE LEGENDS

### Figure 1 Legend.

Reliability data for Magnetic Resonance Arterial Spin Labeling between two measures of the relative dispersion (standard deviation of signal intensity/mean) of perfusion heterogeneity obtained 10 minutes apart within a single testing session in 45 healthy nonsmoking subjects.

### Figure 2 Legend.

Arterial saturation of hemoglobin (SpO<sub>2</sub>, top Panel) and heart rate (bottom panel) in HAPE-Susceptible (●), HAPE-Resistant (□) and Unselected (△) subjects, before and during 30 minutes of exposure to hypoxia (FIO<sub>2</sub> = 0.125). Hypoxia decreases SpO<sub>2</sub> and increases heart rate, \*, p<0.0001 in all 3 groups of subjects.

### Figure 3 Legend

Relative dispersion (bottom panel) in HAPE-Susceptible (●), HAPE-Resistant (□) and Unselected (△) subjects, breathing room air and during 30 minutes of exposure to hypoxia (FIO<sub>2</sub> = 0.125). Relative dispersion is increased by hypoxia in HAPE-susceptible but not in HAPE-resistant or Unselected subjects (# = significantly different from pre-hypoxia in HAPE-Susceptible, \* = significantly different from pre-hypoxia and significantly different from HAPE-Resistant and Unselected subjects, P<0.05)

Figure 4 Legend: Change in relative dispersion from baseline versus arterial saturation after 30 minutes of hypoxia. Symbols as for Figure 3. There was a significant linear relationship between relative dispersion and saturation in HAPE-resistant subjects and Unselected subjects (R = -0.60, R<sup>2</sup> = 0.36, P<0.05). Dotted lines represent ±2 standard deviation prediction limit for this relationship in HAPE-resistant subjects and Unselected subjects. In all cases the data from the HAPE-susceptible subjects lie at or above the + 2 SD limits for this relationship.

Figure 5 Legend: Individual relative dispersion data versus arterial saturation for the 5 HAPE-susceptible subjects. In all subjects there is a strong negative correlation for this relationship (R = 0.92, 0.73, 0.88, 0.86, 0.73 for subjects 1-5 respectively.)

Table 1. Subject Descriptive Characteristics.

Group	Age (years)	Gender	Elevation Of HAPE	Highest Elevation (M)	Height (cm)	Weight (Kg)	FVC (l)	%	FEV1 (l)	%
HAPE- Susceptible	35	F	4023	5883	165.7	59.5	3.12	82	2.44	76
	33	M	4389	4389	175.2	79.5	4.85	94	3.61	84
	31	M	4389	6949	169.5	65.0	4.66	95	4.07	99
	38	M	4267	4267	180.3	98.2	6.52	122	5.35	123
	21	M	3078	3078	170.2	70.0	5.55	109	4.69	108
Means	31.6		4029	5907	172.1	74.4	4.94	100	4.03	98
±SEM	±2.2		±244	±678	±2.5	±6.7	±0.56	±8	±0.49	±8
HAPE- Resistant	33	M	-	8848	191.8	73.5	6.07	99	5.22	105
	35	F	-	6553	165.1	63.6	3.59	96	3.24	102
	30	F	-	6706	162.6	62.7	4.72	126	4.13	129
	40	M	-	6187	177.8	75.0	5.26	102	4.30	103
	24	F	-	5486	162.6	51.4	4.52	117	4.04	120
	34	M	-	6706	175.2	70.5	5.65	112	4.73	105
Means	32.7		-	6736 *	172.5	66.1	4.94	109	4.28	111
±SEM	±2.2			±460	±4.6	±3.6	±0.36	±5	±0.27	±4
Unselected	35	F	-	3597	170.2	72.7	4.72	118	3.76	112
	22	M	-	3962	175.3	70.5	5.33	102	4.49	102
	32	M	-	4328	175.2	68.2	5.86	113	4.53	106
	25	M	-	2438	167.6	55.9	3.95	86	3.37	86
	32	M	-	3048	185.4	84.9	6.04	105	3.90	107
	24	M	-	2682	172.7	66.8	4.95	95	4.18	96
Means	28.3		-	3322	174.4	69.8	5.14	103	4.04	101
±SEM	±2.8			±299	±2.5	±3.8	±0.31	±5	±0.18	±4

Legend for Table 1.\*

= significantly different between groups  $p < 0.05$ . % = percent of predicted values, FVC = forced vital capacity, FEV<sub>1</sub> = forced expiratory volume in one second

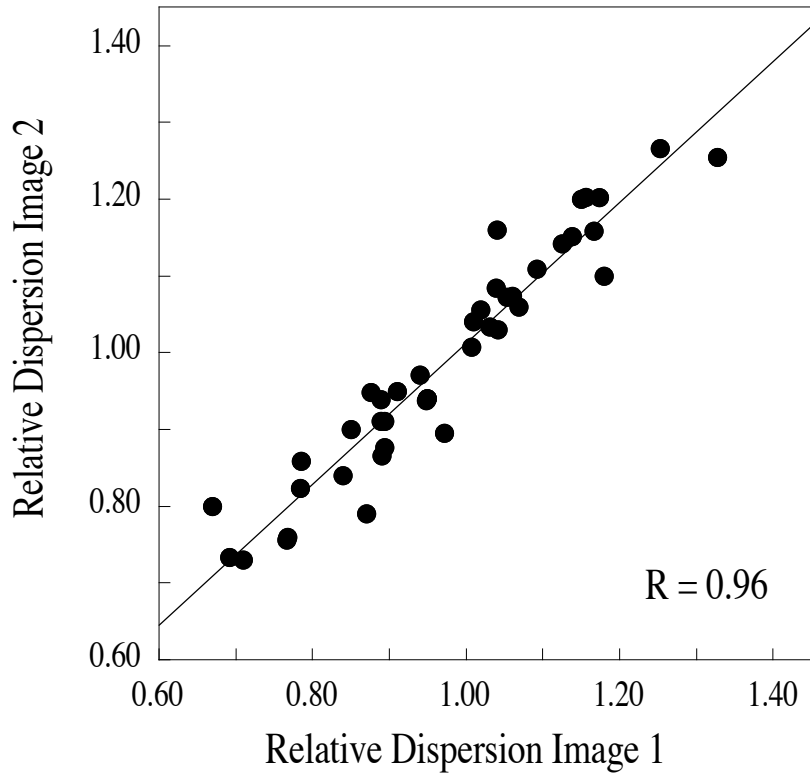


Figure 1

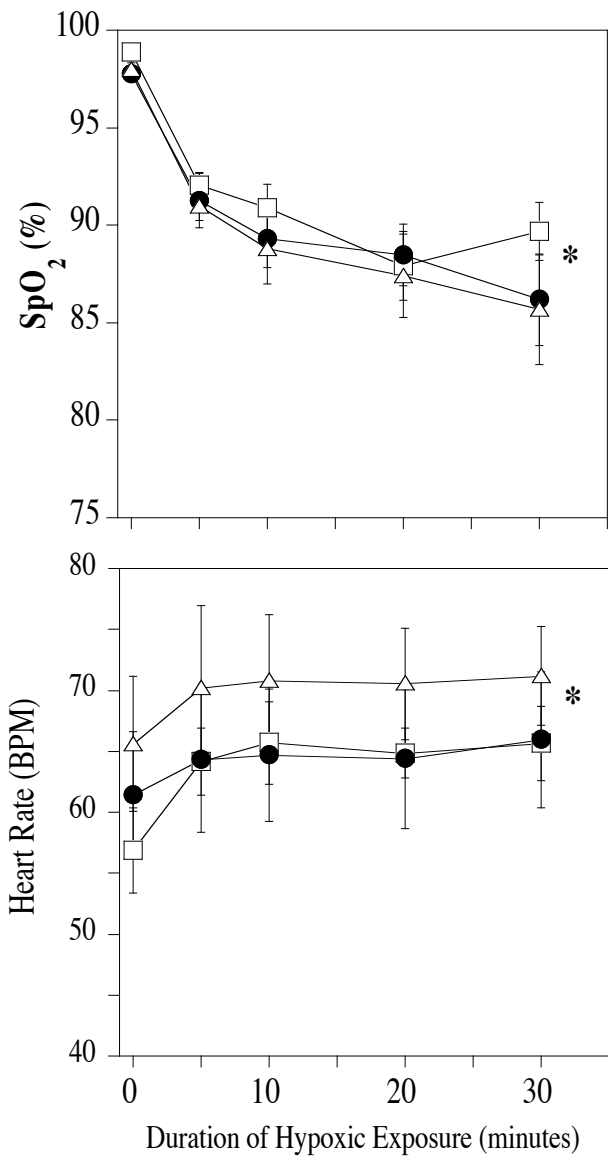
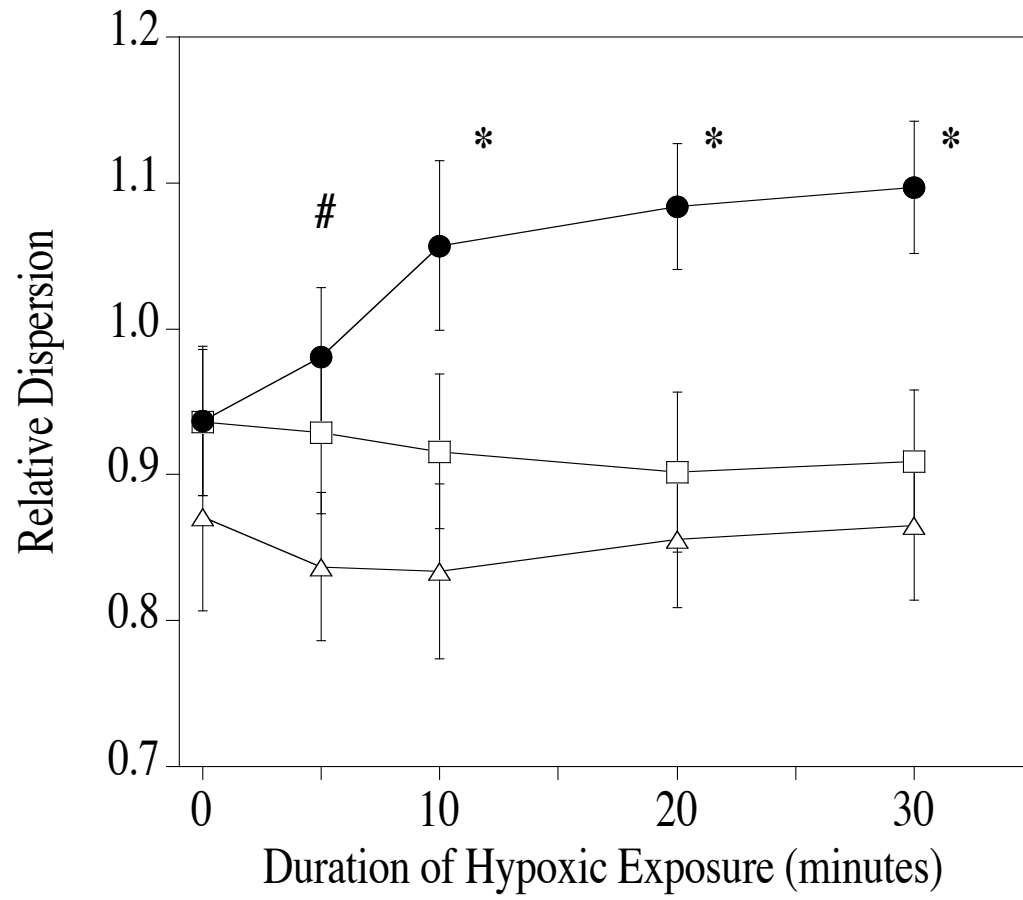


Figure 2



**Figure 3**

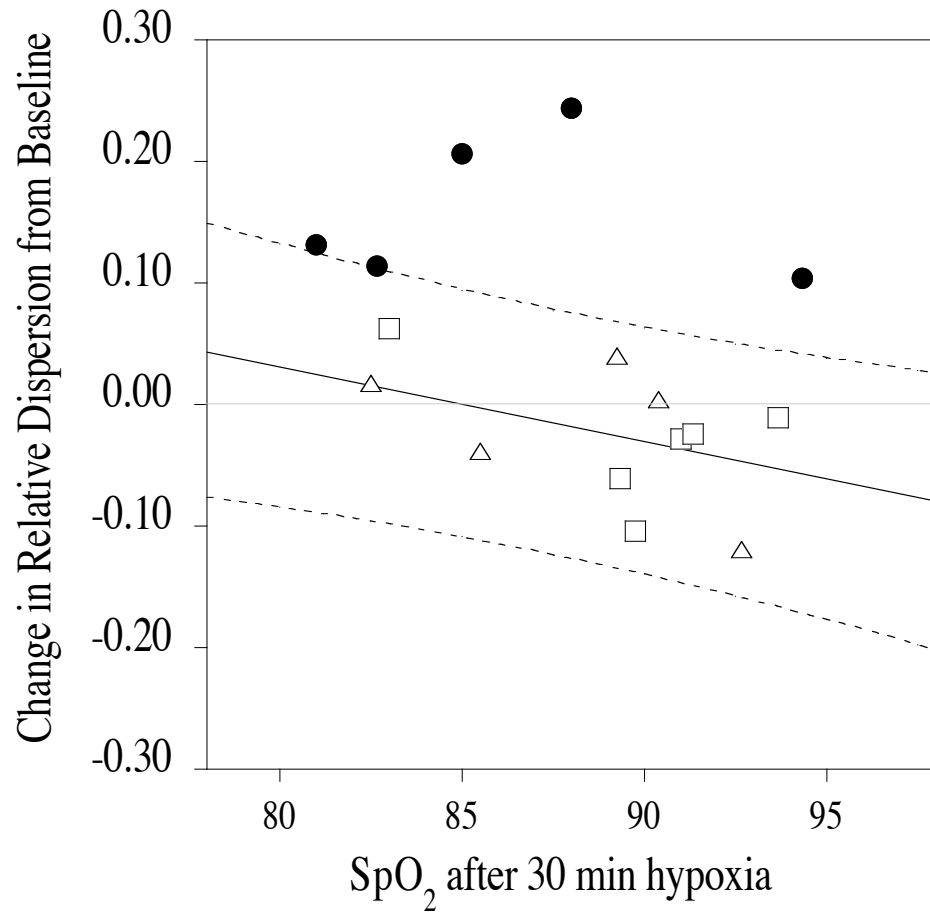


Figure 4

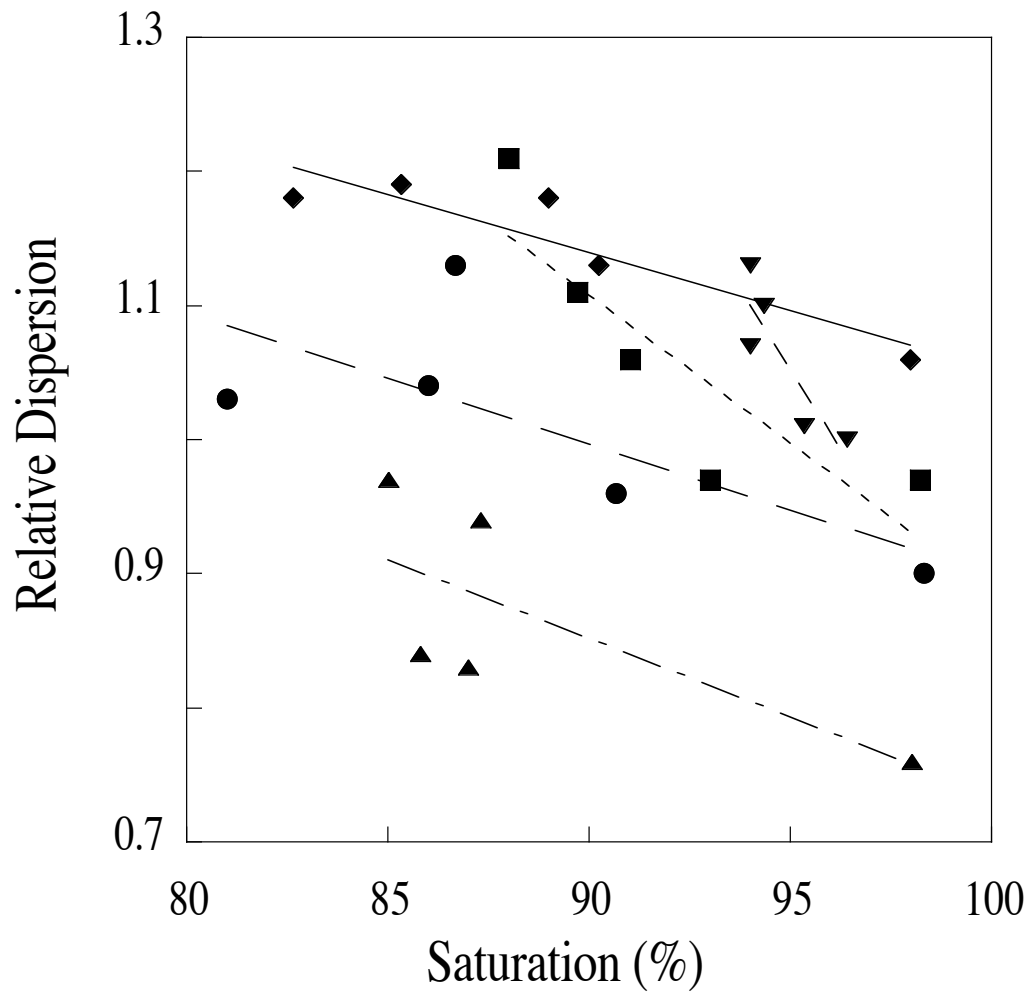


Figure 5

## **EXPANDED METHODS FOR ONLINE DATA SUPPLEMENT**

### **PULMONARY BLOOD FLOW HETEROGENEITY DURING HYPOXIA AND HIGH ALTITUDE PULMONARY EDEMA**

Susan R. Hopkins MD, PhD, Joy Garg MD, Divya S. Bolar BS, Jamal Balouch BS, David L. Levin MD, PhD

## **MRI Arterial Spin Labeling quantification of regional pulmonary blood flow**

Data were collected using a 1.5 tesla (T) MRI scanner (Siemens Vision, Siemens AG, Erlangen, Germany). Arterial spin labeling (ASL) magnetic resonance imaging (MRI) techniques qualitatively and quantitatively evaluate regional pulmonary perfusion by characterizing the rate of arterial blood delivery to a single voxel in the imaged slice of interest. Arterial spin labeling creates a magnetically tagged bolus, by the use of specialized radiofrequency pulses to invert the magnetization of water protons in arterial blood. This tagged water acts as a freely diffusible endogenous tracer, and yields a perfusion-weighted image map (see Figure E1).

Arterial spin labeling has been widely applied to measure cerebral blood flow (E1), and to a lesser extent has been used to evaluate perfusion in skeletal muscle (E2), heart (E3), kidney (E4), and lung(E5). The signal intensity of the image obtained using the arterial spin labeling technique has been shown to be proportional to bulk flow *in vitro* using a tube-flow model (E6) and it has been validated in heart (E3) with microspheres, and skeletal muscle with venous occlusion plethysmography (E7) with an excellent linear relationships between arterial spin labeling measurements and the validating technique. Arterial spin labeling offers high spatial resolution (see below), is completely noninvasive, and can be repeated over short intervals in the same subject. Flow-sensitive Alternating Inversion Recovery with an Extra Radiofrequency pulse (FAIRER) is a recent arterial spin labeling technique that has been used for qualitative and quantitative perfusion imaging (E5, 8).

A custom ASL-FAIRER pulse sequence with a half Fourier acquisition single-shot turbo spin-echo (HASTE) imaging scheme was used to assess pulmonary blood flow heterogeneity as previously described (E5, 8). This turbo spin-echo MR imaging sequences is well-suited for the lung, as it reduce susceptibility effects caused by inhomogeneous magnetic fields (E9), maximizes the intrinsically low lung signal by allowing recovery of  $T_2$  signal loss (E10), and eliminates artifacts caused by respiratory and cardiac motion (E11). Half Fourier acquisition adds an additional two-fold decrease in imaging time, allowing sub-second image acquisition.

A schematic diagram of the ASL-FAIRER lung imaging sequence used (E8) is shown in Figure E2. In order to make the arterial spin labeling images used in this study, two cardiac gated

images were triggered from the beginning of systole (QRS complex) and taken approximately 4 seconds apart during a single apnea at functional residual capacity. After a variable delay time,  $T_{ecg}$ , (see Figure E2) an inversion radio-frequency (RF) pulse (an RF pulse that completely inverts the net magnetization of protons - a 180 degree flip) was applied to the entire volume of the lungs (termed a non-selective tag). The time,  $T_{ecg}$ , was adjusted so that the tag occurred during diastole. The first image (non-selective image) was then obtained following an additional delay,  $T_I$ , so that imaging occurred during the subsequent diastole. After a 4 second delay to allow the protons to re-align with the magnetic field, the same process was repeated to produce the second image. However, for this second image, the inversion pulse was applied only to the region of the lung that contained the imaging slice (termed a selective tag). This selective tag, applied during diastole using the same timing as that used during the non-selective image, acquires an image during the next diastole (following  $T_I$ ). In this case, during  $T_I$ , protons in blood that enter the imaging plane were missed by the selective tag and so will contribute to the image signal in the subtracted image. Protons from stationary structures within the image plane are inverted in both images and therefore do not contribute to the signal in the subtracted image. However protons that are moving (i.e. those in flowing blood) from outside the region of the selective tag that move into the imaging plane will show up as bright in the image. The selective and non-selective images are then subtracted, and the resulting difference in signal from each image voxel is proportional to the amount of blood that entered that voxel from outside the region of the selective tag during the time,  $T_I$ .

### **Data collection**

Subjects were imaged in the supine position using a phased-array torso coil. Imaging was performed at functional residual capacity, to increase the signal to noise characteristics of the image by increasing the amount of tissue relative to air within the lungs. Following a minor amount of training, subjects were able to reliably suspend ventilation at this level, as assessed by the level of the diaphragm on the non-subtracted images, and remained at a stable level for the 8-10 seconds required for the acquisition of the two images. The imaging plane was a single, 15mm thick, coronal slice, that was chosen from an initial series of scout images and located within the posterior lung in line with the posterior descending aorta. The coronal slice was chosen to avoid the heart and large central vessels. An imaging delay time of 700-800 msec was used, equal to 80% of the R-R interval and was kept constant for each subject. Additional MR

parameters were echo time (TE) = 36 msec, flip angle = 30°, NEX = 1, and image matrix = 128X256. The slice field of view (FOV) was 40cm x 40cm, and kept constant for each time point and each subject. Thus, each voxel had a fixed dimension of approximately 1.5 x 3 x 15 mm (~70 mm<sup>3</sup>). All sequence parameters were kept within the established FDA safety guidelines for routine clinical MR examinations.

**Figure E1** shows a pulmonary perfusion image from a healthy subject obtained using this arterial spin labeling technique. Three images are shown: the selective tagged image, the non-selective tagged image, and the subtracted (perfusion weighted) image. The signal intensity of each voxel in the perfusion map is proportional to blood flow.

### **Quantification of perfusion heterogeneity**

MR image data was analyzed using the MATLAB software environment (The Mathworks Inc, Natick, MA). The relative dispersion (also known as the coefficient of variation) of blood flow, defined as the standard deviation of signal intensity divided by the mean signal, for the given region of interest within the lung was used to calculate perfusion heterogeneity. This was done by manually outlining the lung on the un-subtracted image and using this region to define an image mask for the subtracted image. Then mean signal intensity and standard deviation was measured for all voxels within this region of interest, and relative dispersion calculated. The reader is referred to an excellent review of the topic of measuring heterogeneity in the lung by Glenny (E12). It should be noted that relative dispersion measures heterogeneity on a global scale, without considering the spatial location of changes, thus flow to a particular lung region could decrease significantly and if there was a corresponding increase in another lung region, the relative dispersion might not change.

## REFERENCES

- E1. Wong EC, Buxton RB, Frank LR. Quantitative imaging of perfusion using a single subtraction (QUIPSS and QUIPSS II). *Magn Reson Med* 1998;39:702-708.
- E2. Frank LR, Wong EC, Haseler LJ, Buxton RB. Dynamic imaging of perfusion in human skeletal muscle during exercise with arterial spin labeling. *Magn Reson Med* 1999;42:258-267.
- E3. Poncelet BP, Koelling TM, Schmidt CJ, Kwong KK, Reese TG, Ledden P, Kantor HL, Brady TJ, Weisskoff RM. Measurement of human myocardial perfusion by double-gated flow alternating inversion recovery EPI. *Magn Reson Med* 1999;41:510-519.
- E4. Roberts DA, Detre JA, Bolinger L, Insko EK, Lenkinski RE, Pentecost MJ, Leigh JS, Jr. Renal perfusion in humans: MR imaging with spin tagging of arterial water. *Radiology* 1995;196:281-286.
- E5. Mai VM, Berr SS. MR perfusion imaging of pulmonary parenchyma using pulsed arterial spin labeling techniques: FAIRER and FAIR. *J Magn Reson Imaging* 1999;9:483-487.
- E6. Andersen IK, Sidaros K, Gesmara H, Rostrup E, Larsson HB. A model system for perfusion quantification using FAIR. *Magn Reson Imaging* 2000;18:565-574.
- E7. Raynaud JS, Duteil S, Vaughan JT, Hennel F, Wary C, Leroy-Willig A, Carlier PG. Determination of skeletal muscle perfusion using arterial spin labeling NMRI: validation by comparison with venous occlusion plethysmography. *Magn Reson Med* 2001;46:305-311.

- E8. Mai VM, Hagspiel KD, Christopher JM, Do HM, Altes T, Knight-Scott J, Stith AL, Maier T, Berr SS. Perfusion imaging of the human lung using flow-sensitive alternating inversion recovery with an extra radiofrequency pulse (FAIRER). *Magn Reson Imaging* 1999;17:355-361.
- E9. Chen Q, Siewert B, Bly BM, Warach S, Edelman RR. STAR-HASTE: perfusion imaging without magnetic susceptibility artifact. *Magn Reson Med* 1997;38:404-408.
- E10. Haacke E, Brown R, Thompson M, Venkatesan R. *Magnetic resonance imaging: physical principles and sequence design*. New York: John Wiley and Sons; 1999.
- E11. Hatabu H, Tadamura E, Prasad PV, Chen Q, Buxton R, Edelman RR. Noninvasive pulmonary perfusion imaging by STAR-HASTE sequence. *Magn Reson Med* 2000;44:808-812.
- E12. Glenny RW. Heterogeneity in the lung: concepts and measures. In: Hlastala MP, Robertson HT, editors. *Complexity in structure and function in the lung*. New York: Marcel Dekker Inc.; 1998. p. 571-609.

## FIGURE LEGENDS

**Figure E1.** Creation of perfusion weighted image from ASL-FAIRER. Subtraction of selective tagged and non-selective tagged images (A and B, respectively) generates a perfusion weighted map (C). In A and C, the pulmonary vessels are identified as bright, tubular structures, many of which are seen to bifurcate to successively smaller vessels. A diffuse blush throughout the lungs in C is seen from flow within the microvasculature. The image is presented with the standard radiographic convention: the patient's left is to the right side of the image. The large, vertically oriented vessel just to the (patient's) left of midline is the aorta.

**Figure E2.** Schematic of ASL-FAIRER image timing. Two such images, one using a nonselective inversion pulse (tag) and the second using a selective inversion pulse, are acquired separated by a 4 second delay (see text for details). T<sub>ecg</sub> is the time between the QRS complex and the application of the inversion pulse. TI is the time between the inversion pulse and the image acquisition.

**Figure E1**

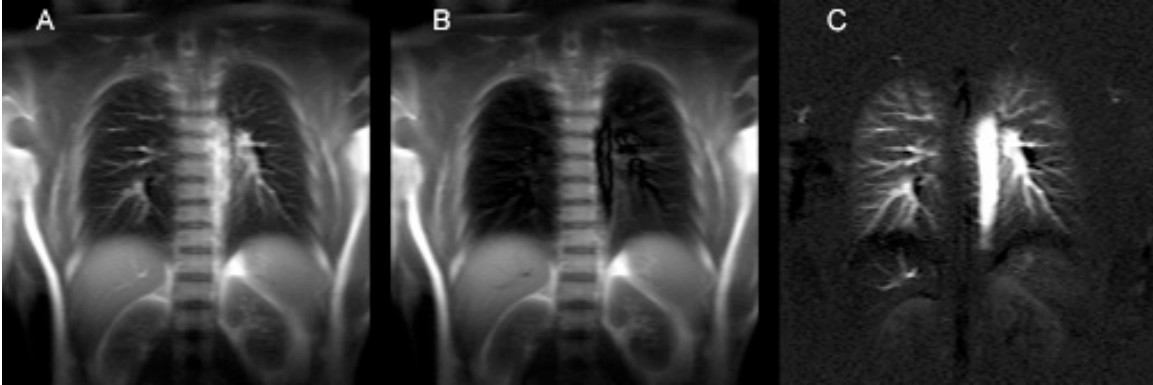


**Figure E2**

